

Low-Reset-Current Ring-Confined-Chalcogenide Phase Change Memory

You Yin* and Sumio Hosaka

Graduate School of Engineering, Gunma University, Kiryu, Gunma 376-8515, Japan

Received February 10, 2012; revised July 4, 2012; accepted July 17, 2012; published online September 20, 2012

In this study, we proposed a ring-shaped confined chalcogenide (RCC) phase change memory (PCM) cell to reduce the reset current compared with a conventional normal bottom contact (NBC) cell and a conventional normal confined chalcogenide (CC) cell. The finite element analysis of the proposed RCC cell was systematically conducted depending on the radius of the center SiO₂ cylinder, surrounded by the phase change material. The highest temperature at different programming currents markedly increases by increasing the radius of the SiO₂ cylinder. On the basis of the simulated relationships between the cell resistance and the programming current, it was demonstrated that the derived reset current of the RCC cell can be reduced to 41% of that of the conventional NBC PCM cell. © 2012 The Japan Society of Applied Physics

1. Introduction

Nowadays, there is a growing demand for nonvolatile memories, which are widely used in our daily lives. They are used in notebook computers, digital cameras, and smart phones to store photographs and other important information. In recent years, many prospective memories have been intensively researched because the current mainstream flash memory has serious problems such as its low scalability and low speed. Recently, these emerging memories have included the single-electron memory,¹⁻³⁾ nanocrystal memory,⁴⁾ ferroelectric random access memory (FeRAM),⁵⁾ magnetoresistive random access memory (MRAM),⁶⁾ phase change random access memory (PRAM or PCM),⁷⁻⁹⁾ resistive random access memory (RRAM),¹⁰⁻¹²⁾ and atomic switch.¹³⁾

In the above-mentioned memories, PCM is widely regarded as the best candidate for next-generation nonvolatile memories. It is a type of nonvolatile RAM that stores data by changing the state of the material used between the amorphous and crystalline states at the microscopic level. PCM is 500 to 1,000 times faster than a normal flash memory. PCM exhibits many merits such as its nonvolatile operation, high speed, low cost, multilevel storage, excellent endurance to cycling, great scalability, superior radiation tolerance, and good compatibility with silicon fabrication processes.¹⁴⁻¹⁷⁾

The high reset current of PCM is one of the biggest obstacles for its mass production. For instance, it is 1.2–1.5 mA for a PCM cell with a technological node of 180 nm. Solutions to reduce the operation current, therefore, attract much attention worldwide. One of the most important solutions is to adopt some phase change materials with a relatively high resistivity to improve the heat efficiency of a PCM cell via self Joule heating. For example, the resistivity of phase change materials can be markedly increased by doping with N,¹⁸⁾ C,¹⁹⁾ O,²⁰⁾ and other elements or by cosputtering^{21,22)} with an insulator such as SiO₂. The other effective solution is to optimize the cell structure. Ha *et al.* reported an edge contact PRAM cell and Varesi *et al.* proposed a μ -trench architecture to reduce reset current.^{23,24)} However, the fabrication of these memory cells is much more complicated, and the area of these cells is larger than that of the corresponding normal bottom contact (NBC) cell. In this study, a ring-shaped confined chalcogenide (RCC)

cell structure is proposed and analyzed thermally and electrically by two-dimensional finite element analysis. This type of cell has a simple architecture and can be fabricated easily. Energy generated by Joule heating could be more efficiently used to obtain a smaller programming volume for the RCC cell than for the NBC cell and normal confined chalcogenide (CC) cell;^{25,26)} thus, the reset current of the RCC cell will remarkably decrease below half of that of the NBC cell.

In this work, we systematically investigate the temperature distribution and cell resistance as functions of the programming current in our proposed RCC cell by finite element analysis compared with the NBC and CC cell structures.

2. Modeling of PCM

2.1 Principle of PCM and mathematical model

By applying a high and short electrical pulse to a PCM cell, the programming volume of a chalcogenide alloy is heated to a temperature above its melting point (T_m), and then the formerly melted part is quenched below the crystallization temperature (T_c) so rapidly that crystallization is sufficiently prevented. The PCM cell then enters a highly resistive amorphous state (reset state), which could be used as the logic “1” for binary storage. On the other hand, when a low and long electrical pulse is applied to heat a chalcogenide alloy to a temperature between T_m and T_c , the programmable volume of the chalcogenide alloy layer crystallizes, and thus, a low-resistivity crystalline state (namely, set state as the logic “0”) could be written into the cell.

The temperature profile within a body depends on the rate of its internally generated heat, its capacity to store some of this heat, and its rate of thermal conduction to its boundaries (where heat is transferred to the surrounding environment). Mathematically, this is stated by the heat equation

$$\rho C \frac{\partial T}{\partial t} - \nabla \cdot (k \nabla T) = Q_h, \quad (1)$$

where ρ is the density, T is the temperature, C is the heat capacity, k is the thermal conductivity, t is the time, and Q is the heat flux.

The heat generated by Joule heating Q is given by

$$Q = \frac{1}{\sigma} |J|^2 = \sigma |\nabla V|^2, \quad (2)$$

where σ is the electric conductivity, J is the electric current density, and V is the electric potential.

*E-mail address: yinyou@gunma-u.ac.jp

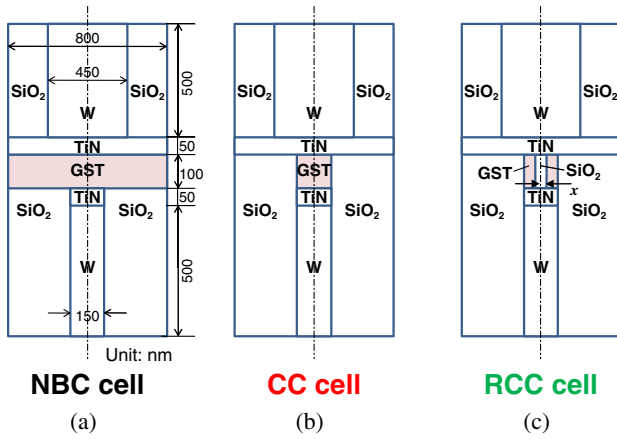


Fig. 1. (Color online) Simulation models: (a) Conventional NBC PCM cell. (b) CC PCM cell. (c) Proposed RCC PCM cell with a center SiO₂ cylinder surrounded by phase change material. The SiO₂ cylinder has a radius of x and the corresponding RCC cell is called RCC- rx .

Table I. Physical properties of materials used in simulation.

Material	Melting point T_m (K)	Density ρ (kg/m ³)	Specific heat C (J kg ⁻¹ K ⁻¹)	Thermal conductivity κ (W m ⁻¹ K ⁻¹)	Electrical conductivity ρ_{elec} (Ω m)
c-Ge ₂ Sb ₂ Te ₅	905	6200	202	0.46	3.6×10^{-4}
Contact TiN	3223	5240	784	22	2×10^{-7}
Heater TiN	3223	5240	784	0.44	1×10^{-5}
W	3680	19300	132	174	5.39×10^{-8}
SiO ₂	1873	2330	1330	1.4	1.0×10^{14}

2.2 Finite element models of PCM cells

Equation (1) is solved by finite element analysis in this paper. The NBC, CC, and RCC cells are shown in Figs. 1(a)–1(c), respectively. The NBC cell shown in Fig. 1(a) is assumed to have a Si substrate/W plug/TiN resistive heater/GST/TiN contact/W layered structure, and the thicknesses of each layer from the W plug are 500, 50, 100, 50, and 500 nm, respectively. The diameter of the TiN resistive heater is 150 nm. The TiN contact and W layers are taken to be a diffusion barrier and a metal plug material, respectively.²⁷⁾ The CC memory cell shown in Fig. 1(b) has the same size of GST chalcogenide as the TiN resistive heater and W-plug. Therefore, we call such a cell a confined chalcogenide structure. Furthermore, the confined chalcogenide was used to partially fill a SiO₂ cylinder of x radius (nm). Thus, the chalcogenide had the shape of a ring, as shown in Fig. 1(c). This structure is hereafter called the RCC- rx cell in this paper. The physical properties of the materials used in the simulation are summarized in Table I.

3. Simulation Results and Discussion

The temperature distribution is very important for understanding the operation physics of a PCM cell. To reset such a cell to a high-resistance amorphous state, it is necessary to partially heat the phase change layer above its melting point. The temperature distributions of the researched cells in such a case are shown in Fig. 2. A 30 ns pulse for reset operation was applied to these cells. It should be noted that only half of

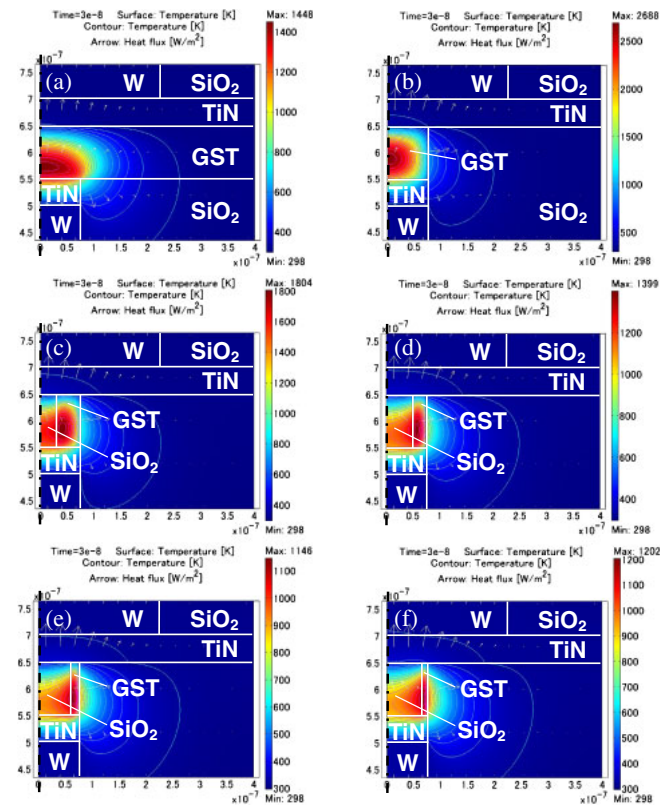


Fig. 2. (Color online) Temperature distributions of cells due to 30-ns-pulse reset operation. (a) NBC cell at 1.1 mA. (b) CC cell at 0.9 mA. (c) RCC-r30 cell at 0.8 mA. (d) RCC-r50 cell at 0.65 mA. (e) RCC-r60 cell at 0.5 mA. (f) RCC-r65 cell at 0.45 mA.

the cross-sectional temperature distribution is shown here for each cell. The dash-dotted line is a symmetric axis for each structure. Figure 2(a) shows the temperature distribution of the NBC cell after applying a 1.1 mA, 30 ns pulse. As we can see, the high-temperature region looks like a semiellipse. This is in good agreement with the experimental results.²⁸⁾ The temperature distribution of the CC cell after applying a 0.9 mA, 30 ns pulse is shown in Fig. 2(b). As we can see, the high-temperature region becomes a semicircle. Clearly, even a low current of 0.9 mA can induce a high temperature compared with the case for the NBC cell. Figure 2(c) shows the temperature distribution of the RCC-r30 cell with a SiO₂ cylinder that has a radius of 30 nm. A 0.8 mA, 30 ns pulse was applied to the cell. The high-temperature region was markedly reduced in size compared with those in both the NBC and CC cells. The temperature distribution of the RCC-r50 cell shown in Fig. 2(d) is very similar to that of the RCC-r30 cell, but a low pulse of 0.65 mA was required to amorphize the RCC-r50 cell. The high-temperature region further concentrates in the GST rings when the radius of the SiO₂ cylinder increases to 60 nm and then to 65 nm, as shown in Figs. 2(e) and 2(f).

The amorphized region was investigated with increasing pulse amplitude for each cell. The shape of the amorphized region of the NBC cell looks like a semiellipse. The size of the semiellipse gradually increases with increasing pulse amplitude from 0.9 to 1.5 mA, as shown in Figs. 3(a)–3(c). The amorphized region of the CC cell grows in size from a semicircle, and finally the entire GST region changes to the

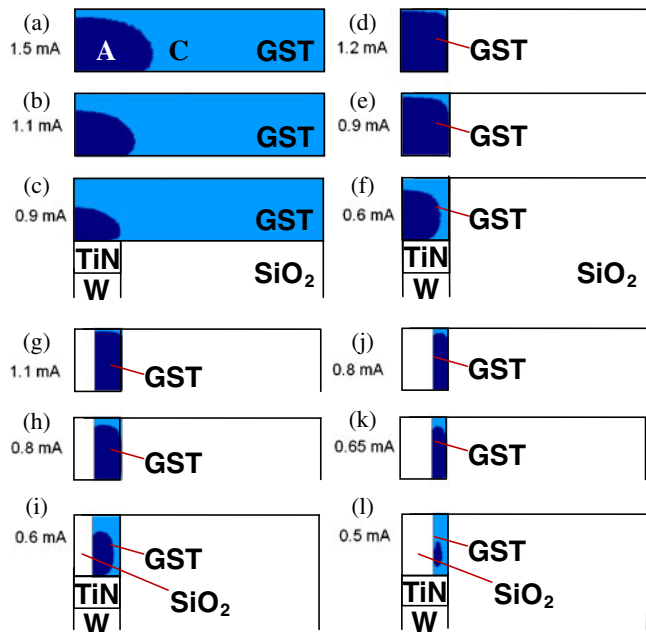
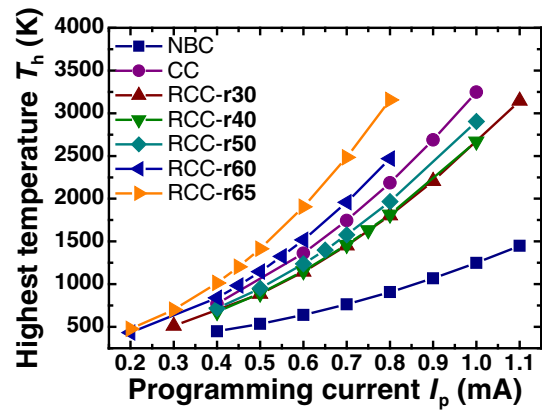


Fig. 3. (Color online) Amorphization processes of PCM cells at different programming currents. (a–c) NBC cell at 1.5, 1.1, and 0.9 mA. (d–f) CC PCM cell at 1.2, 0.9, and 0.6 mA. (g–i) RCC-r30 PCM cell at 1.1, 0.8, and 0.6 mA. (j–l) RCC-r50 PCM cell at 0.8, 0.65, and 0.5 mA.

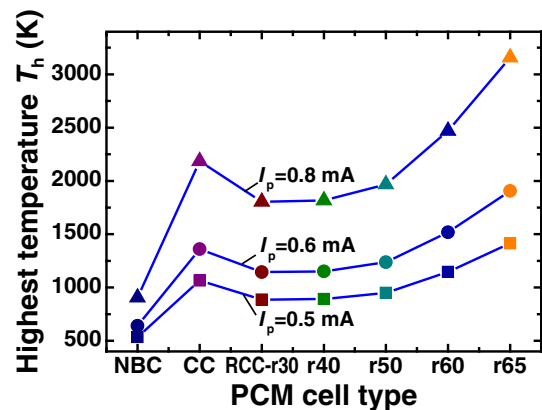
amorphous phase with increasing applied pulse amplitude from 0.6 to 1.2 mA, as shown in Figs. 3(d)–3(f). An ear-shaped amorphized region in the RCC-r30 cell formed after applying a 0.6 mA pulse, as shown in Fig. 3(i). Increasing the pulse amplitude induces an enlargement of the amorphized region, as shown in Figs. 3(g) and 3(h), and the GST region finally becomes amorphous after applying a 1.1 mA pulse. The application of a 0.5 mA pulse starts amorphization in the RCC-r50 cell and the small amorphized region has the shape of a water drop, as shown in Fig. 3(l). Like that in the RCC-r30 cell, this amorphized region becomes larger with increasing pulse amplitude up to 0.8 mA, as shown in Figs. 3(j) and 3(k).

The highest temperature T_h in the GST region as a function of the programming current I_p for each cell is summarized in Fig. 4(a). Clearly, T_h increases with I_p for each cell. It can be clearly seen that T_h for the conventional NBC cell is much lower than those for the other cells. The RCC-r65 cell has the greatest T_h at different programming currents among the cells. The CC cell has an intermediate T_h among these cells. The T_h 's of the proposed cells were compared with that of the conventional CC cell, as shown in Fig. 4(b). Squares, circles, and triangles represent the T_h 's of these cells induced by pulses with amplitudes of 0.5, 0.6, and 0.8 mA, respectively. T_h generally increases with increasing radius of the center SiO₂ cylinder from 30 to 65 nm. In particular, a clear increase in T_h can be observed from the RCC-r50 cell to the RCC-r60 cell. From the T_h 's of these cell types, it can be found that the CC cell has a T_h between those of the RCC-r50 and RCC-r60 cells at each programming current.

The simulated relationships between the device resistance and programming current of the NBC and the proposed CC and RCC cells are plotted in Fig. 5(a). As described in



(a)



(b)

Fig. 4. (Color online) (a) Highest temperature in GST as a function of the programming current of PCM cells. (b) Highest temperatures induced by 0.5, 0.6, and 0.8 mA pulses for each cell.

ref. 27, the total circuit resistance R_c is within 1000–1500 Ω . Here, R_c is taken to be 1000 Ω . The simulated reset current of the NBC cell is approximately 1.1 mA, which is in good agreement with the reported experimental results. The reset current of the CC cell reduces to approximately 900 μ A. Thus, by adopting the proposed CC PCM cell, the operation current could be successfully reduced to below 1 mA for low-power memories. Furthermore, the R – I_p curves of RCC cells are shown on the left-hand side in Fig. 5(a). Clearly, these curves gradually shift to the upper left-hand side with increasing radius of the center SiO₂ cylinder from 30 to 65 nm. For all of the cells, the resistance changes by about 3 orders of magnitude owing to the reset operation, i.e., GST amorphization. Figure 5(b) shows the reset voltages and reset powers the different PCM cell types. As we can see, the necessary power decreases with increasing radius of the center SiO₂ cylinder for the RCC cells although the reset voltage increases. The reset currents of the proposed cells are compared with that of the conventional NBC cell, as shown in Fig. 5(c). The reset current of the CC cell is 1.1 mA, regarded as 100%. For the CC cell, the reset current can decrease to 900 μ A; it is 82% of that of the CC cell. The RCC-r30 cell has a lower reset current of 800 μ A, which is 72% of that of the NBC cell. The reset current of the RCC cells further decreases with increasing radius of the center SiO₂ cylinder from 30 to 65 nm. The reset currents of the

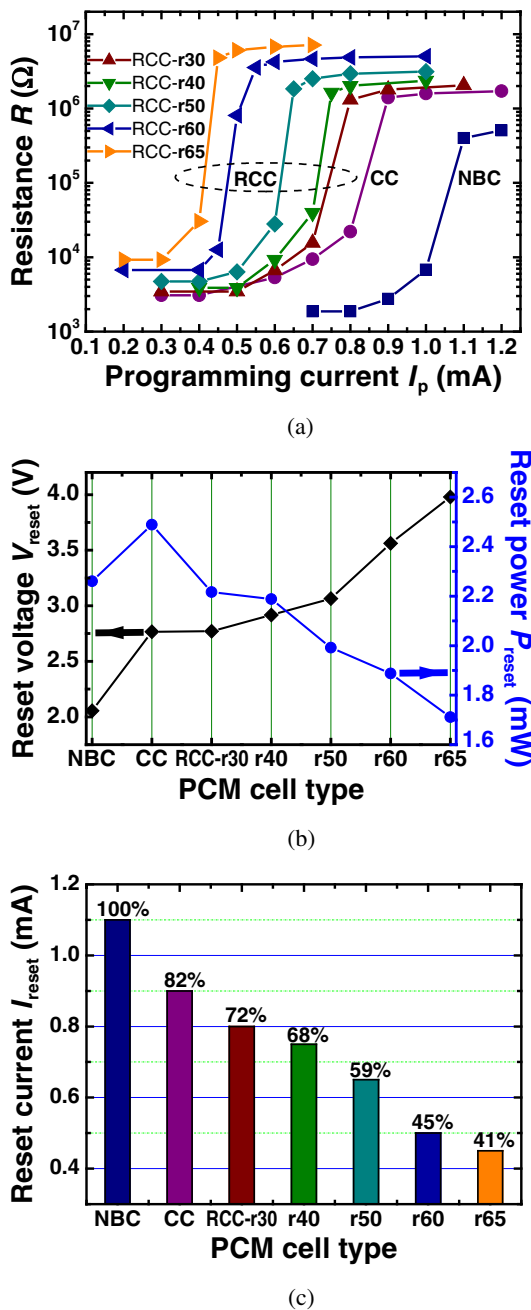


Fig. 5. (Color online) (a) Device resistance as a function of the programming current of PCM cells. (b) Reset voltage and power vs PCM cell type. (c) Reset current vs PCM cell type.

RCC-r60 and RCC-r65 cells can even decrease to 45 and 41% of that of the NBC cell, respectively. The result shows that the proposed RCC cell structure has a low reset current and a low power consumption and is therefore very promising for future mass production.

The proposed RCC cell is thought to be easier to fabricate than the low-current μ -trench cell. For our proposed RCC cell, only one step of lithography for the formation of the center SiO_2 cylinder is required from the fabrication of the bottom heater to the fabrication of the top TiN electrode. However, three steps of lithography for the formation of two square heaters, the oxide in the heater for the μ -trench, and the contact area between GST and the heater are necessary for the μ -trench cell.^{29,30} There are still some technical

issues to be solved to practically fabricate the proposed cell in the future. For example, chemical mechanical polishing (CMP) for GST and the removal of the bottom GST in the contact hole are necessary after depositing the layer of GST.

In this work, we proposed an RCC cell with a reduced thickness of the GST wall layer up to 10 nm. It was reported that PCM can still work well using a layer of GeSb with a thickness of 3 nm.³¹ Therefore, we think that there is still room for further reducing the reset current.

4. Conclusions

We systematically investigated our proposed RCC cell structure and compared it with a conventional NBC cell and our previously proposed CC cell by finite element analysis. The following conclusions were drawn on the basis of the comparison of the temperature distributions and resistances at different programming currents of the NBC and CC cells.

- (1) The highest temperature of the RCC cell is much higher than that of the NBC cell. The highest temperature increases with increasing radius of the center SiO_2 cylinder from 30 to 65 nm.
- (2) The size of the amorphized region can be markedly reduced by adopting the RCC cell, instead of the NBC and CC cells.
- (3) The reset of the proposed RCC cell could be operated at a low current, below half of the reset current for the conventional NBC cell, allowing the realization of low-power high-density memory.

Acknowledgements

This work was financially supported by a Grant-in-Aid for Young Scientists (No. 24686042) and a Grant-in-Aid for Scientific Research (No. 24360003) from the Ministry of Education, Culture, Sports, Science and Technology of Japan.

- 1) T. Fujiaki, K. Ohkura, and A. Nakajima: *Jpn. J. Appl. Phys.* **47** (2008) 4985.
- 2) Y. Yin, J. F. Jiang, Q. Y. Cai, and B. C. Cai: *Chin. J. Electron.* **12** (2003) 451.
- 3) W. Xuan, A. Beaumont, M. Guilmain, M. A. Bounouar, N. Baboux, J. Etzkorn, D. Drouin, and F. Calmon: *IEEE Trans. Electron Devices* **59** (2012) 212.
- 4) D. D. Jiang, Z. L. Huo, M. H. Zhang, L. Jin, J. Bai, Z. A. Yu, J. Liu, Q. Wang, X. N. Yang, Y. Wang, B. Zhang, J. N. Chen, and M. Liu: *Semicond. Sci. Technol.* **26** (2011) 115008.
- 5) B. Lei, C. Li, D. H. Zhang, Q. F. Zhou, K. K. Shung, and C. W. Zhou: *Appl. Phys. Lett.* **84** (2004) 4553.
- 6) S. V. Pietambaram, N. D. Rizzo, R. W. Dave, J. Goggin, K. Smith, J. M. Slaughter, and S. Tehrani: *Appl. Phys. Lett.* **90** (2007) 143510.
- 7) D. S. Chao, C. H. Lien, C. M. Lee, Y. C. Chen, J. T. Yeh, F. Chen, M. J. Chen, P. H. Yen, M. J. Kao, and M. J. Tsai: *Appl. Phys. Lett.* **92** (2008) 062108.
- 8) Y. Yin, A. Miyachi, D. Niida, H. Sone, and S. Hosaka: *Jpn. J. Appl. Phys.* **45** (2006) L726.
- 9) Y. Yin, T. Noguchi, and S. Hosaka: *Jpn. J. Appl. Phys.* **50** (2011) 105201.
- 10) M. J. Rozenberg, I. H. Inoue, and M. J. Sanchez: *Phys. Rev. Lett.* **92** (2004) 178302.
- 11) Y. Watanabe, J. G. Bednorz, A. Bietsch, Ch. Gerber, D. Widmer, A. Beck, and S. J. Wind: *Appl. Phys. Lett.* **78** (2001) 3738.
- 12) H. Y. Lee, P. S. Chen, T. Y. Wu, Y. S. Chen, F. Chen, C. C. Wang, P. J. Tzeng, C. H. Lin, M. J. Tsai, and C. H. Lien: *IEEE Electron Device Lett.* **30** (2009) 703.
- 13) K. Terabe, T. Hasegawa, T. Nakayama, and M. Aono: *Nature* **433** (2005) 47.

- 14) J. Feng, Y. F. Lai, B. W. Qiao, B. C. Cai, Y. Y. Lin, T. A. Tang, and B. Chen: *Jpn. J. Appl. Phys.* **46** (2007) 5724.
- 15) Y. Yin, H. Sone, and S. Hosaka: *Jpn. J. Appl. Phys.* **44** (2005) 6208.
- 16) Y. Yin, N. Higano, H. Sone, and S. Hosaka: *Appl. Phys. Lett.* **92** (2008) 163509.
- 17) M. H. R. Lankhorst, B. W. S. M. M. Ketelaars, and R. A. M. Wolters: *Nat. Mater.* **4** (2005) 347.
- 18) Y. Yin, H. Sone, and S. Hosaka: *J. Appl. Phys.* **102** (2007) 064503.
- 19) G. Betti Beneventia, L. Perniola, V. Sousa, E. Gourvest, S. Maitrejean, J. C. Bastien, A. Bastard, B. Hyot, A. Fargeix, C. Jahan, J. F. Nodin, A. Persico, A. Fantini, D. Blachier, A. Toffoli, S. Loubriat, A. Roule, S. Lhostis, H. Feldis, and G. Reimbold: *Solid-State Electron.* **65–66** (2011) 197.
- 20) N. Matsuzaki, K. Kurotsuchi, Y. Matsui, O. Tonomura, N. Yamamoto, Y. Fujisaki, N. Kitai, R. Takemura, K. Osada, S. Hanzawa, H. Moriya, T. Iwasaki, T. Kawahara, N. Takaura, M. Terao, M. Matsuoka, and M. Moniwa: *IEDM Tech. Dig.*, 2005, p. 738.
- 21) S. W. Ryu, J. H. Oh, J. H. Lee, B. J. Choi, W. Kim, S. K. Hong, C. S. Hwang, and H. J. Kim: *Appl. Phys. Lett.* **92** (2008) 142110.
- 22) D. Lee, S. S. Yim, H. K. Lyeo, M. H. Kwon, D. Kang, H. G. Jun, S. W. Nam, and K. B. Kim: *Electrochem. Solid-State Lett.* **13** (2010) K8.
- 23) Y. H. Ha, J. H. Yi, H. Horii, J. H. Park, S. H. Joo, S. O. Park, U.-I. Chung, and J. T. Moon: *Symp. VLSI Technology Dig. Tech. Pap.*, 2003, p. 175.
- 24) E. Varesi, A. Modelli, P. Besana, T. Marangon, F. Pellizzer, A. Pirovano, and R. Bez: presented at EPCOS 04.
- 25) Y. Yin, H. Sone, and S. Hosaka: *Jpn. J. Appl. Phys.* **45** (2006) 6177.
- 26) Y. N. Hwhang, S. H. Lee, S. J. Ahn, S. Y. Lee, K. C. Ryoo, H. S. Hong, H. C. Koo, F. Yeung, J. H. Oh, H. J. Kim, W. C. Jeong, J. H. Park, H. Horii, Y. H. Ha, J. H. Yi, G. H. Koh, G. T. Jeong, H. S. Jeong, and K. Kim: *IEDM Tech. Dig.*, 2003, p. 893.
- 27) D. H. Kang, D. H. Ahn, K. B. Kim, J. F. Webb, and K. W. Yi: *J. Appl. Phys.* **94** (2003) 3536.
- 28) H. S. P. Wong, S. Raoux, S. B. Kim, J. Liang, J. P. Reifenberg, B. Rajendran, M. Asheghi, and K. E. Goodson: *Proc. IEEE* **98** (2010) 2201.
- 29) F. Bedeschi, R. Bez, C. Boffino, E. Bonizzoni, E. C. Buda, G. Casagrande, L. Costa, M. Ferraro, R. Gastaldi, O. Khouri, F. Ottogalli, F. Pellizzer, A. Pirovano, C. Resta, G. Torelli, and M. Tosi: *IEEE Solid-State Circuits* **40** (2005) 1557.
- 30) R. Bez and F. Pellizzer: presented at EPCOS 07.
- 31) S. Raoux, G. W. Burr, M. J. Breitwisch, C. T. Rettner, Y. C. Chen, R. M. Shelby, M. Salinga, D. Krebs, S. H. Chen, H. L. Lung, and C. H. Lam: *IBM J. Res. Dev.* **52** (2008) 465.